Food Chemistry: X 22 (2024) 101363

Contents lists available at ScienceDirect

Food Chemistry: X

journal homepage: www.sciencedirect.com/journal/food-chemistry-x

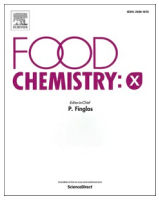

Encapsulation and characterization of ω-3 medium- and long-chain triacylglycerols microencapsulated with different proteins as wall materials

Zhen Yang [a,1], Yujie Guo [a,1], Chili Zeng [a], Fuwei Sun [b], Zhongjiang Wang [b], Weimin Zhang [a], Tian Tian [a], Lingyue Shan [c], Yunxiang Zeng [d], Zhaoxian Huang [a,e,*], Lianzhou Jiang [a,b,e,*]

[a] School of Food Science and Engineering, Hainan University, Haikou 570228, China
[b] College of Food Science, Northeast Agricultural University, Harbin 150030, China
[c] College of Agriculture and Life Sciences, Kangwon National University, Chuncheon 24341, South Korea
[d] Wenzhou Vocational College of Science and Technology, Wenzhou 325000, China
[e] Collaborative Innovation Center of Nanfan and High-Efficiency Tropical Agriculture, Hainan University, Haikou 570228, China

ARTICLE INFO

Keywords:
Encapsulation efficiency
Medium- and long-chain triacylglycerols
Plant protein
Storage stability
Structural lipids microcapsules

ABSTRACT

In this study, ω-3 medium- and long-chain triacylglycerols (MLCTs) microcapsules with excellent performance were obtained using soy protein as the wall component to address the oxidation-related problems of MLCTs. Additionally, the effect of soy, whey, or pea proteins on microcapsules in terms of the changes in their structure and physicochemical properties was investigated. The results showed that the small particle size, low PDI (polydispersity index) and zeta potential, fast adsorption rate, and low interfacial tension of these protein-based samples fabricated through the O/W template method were conducive to maintaining the integrity of microcapsules during spray-drying. The microcapsules, characterized by a spherical shape, exhibited superior encapsulation efficiency of 94.56%, surpassing the findings of previous investigations. Overall, these microcapsules exhibited long-term storage stability and low controllable release rates, which could be utilized as carriers for liposoluble actives.

1. Introduction

As modified fat, structured lipids (SLs) have garnered widespread attention due to their excellent functional properties in the food field (Li & Hui, 2021). Typically, fatty acids are classified as short-chain fatty acids (SCFAs), medium-chain fatty acids (MCFAs), and long-chain fatty acids (LCFAs) based on the number of carbons in their molecules. Medium- and long-chain triacylglycerols (MLCTs), a combination of the medium- and long-chain fatty acids, are novel SLs with unique functions (Huang et al., 2020). The peculiar structure of MLCTs endows them with essential properties that differ from the medium-chain triacylglycerols (MCTs) and long-chain triacylglycerols (LCTs). As such, they are often used as an adequate energy source, offering essential properties for the body (Lai et al., 2023), such as reducing blood lipid levels (Lee, Tang, Chan, Phuah, & Tan, 2021), and improving the weak-side of the MCTs and LCTs by balancing lipid metabolism and decreasing body fat accumulation (Du et al., 2020). The type of oil absorbed and unitized by the human body mainly includes ω-6 lipids, with only a small amount of ω-3 lipids being absorbed and accumulate into the body. In this context, the optimization of absorption can be achieved through deliberate synthesis and intake of ω-3 MLCTs. Nevertheless, addressing the susceptibility of ω-3 lipids to oxidation is imperative to enhance their storage stability.

Recently, the current application forms of MLCTs in medicine and food have attracted widespread attention. Based on the distinctness of liquid state and solid state, the application forms of SLs are divided into emulsion and microcapsule. Lipid microcapsules of solid power state can be obtained by the microencapsulation of emulsion with a diverse ratio of oil to water phase using an emulsifier and the composition of the wall material (Cheng et al., 2024). Several parameters of emulsion states can have a significant impact on their microcapsule properties. Among them, particle size and size distribution of emulsion droplets are the most significant parameters to be controlled before microencapsulation, as the higher encapsulation efficiency of microcapsules is directly associated with the small and monodisperse emulsion droplets. Some studies have shown that the small droplet size is positively correlated with the high encapsulation efficiency (Ramakrishnan et al., 2013).

* Corresponding authors at: School of Food Science and Engineering, Hainan University, Haikou 570228, China.
E-mail addresses: huangzhaoxian@hainanu.edu.cn (Z. Huang), jlzname@163.com (L. Jiang).
[1] Both are co-first authors.

https://doi.org/10.1016/j.fochx.2024.101363
Received 24 February 2024; Received in revised form 26 March 2024; Accepted 4 April 2024
Available online 7 April 2024

Vega et al. found that a decreased droplet size of emulsion could result in encapsulated microcapsule powders with lower content of unencapsulated oil at the particle surface and higher volatile retention (Vega, Kim, Chen, & Roos, 2005). Viscosity is regarded as another important parameter of emulsion, as high viscosity interferes with atomization during microencapsulation, such as spray-drying, leading to the formulation of large elongated droplets (Gharsallaoui, Roudaut, Chambin, Voilley, & Saurel, 2007). In addition, other parameters of emulsion, such as the stability and composition of emulsion, could also affect the properties of microcapsules powders, including the morphology, encapsulation efficiency, surface free oil content, and oxidation stability of microcapsules (Ramakrishnan et al., 2013).

Microencapsulation of MLCTs is the common method for the high-value application of this SLs emulsion. In the microencapsulation process, the SLs emulsions are converted into micro/nano-particles to preserve the initial status of unsaturated fatty acids and encapsulated bioactive during exposure to various ambient conditions (Korma, Wei, Ali, Abed, & Wang, 2018). The stability and bioavailability of the microcapsule depend on its wall material. So far, many materials from different sources have been obtained and utilized as the wall composition of SLs-based microcapsules, mainly including carbohydrates and proteins. Proteins can sustain at the O/W interfaces, stabilizing the emulsion through electrostatic stabilization and forming a thick protective film with good viscoelasticity, which provides protection to the emulsion droplet (Khem, Bansal, Small, & May, 2016). Recently, the application source of proteins for the wall materials of the microcapsule system is focused on single, composite, and modified proteins, including single type (soy protein, pea protein, faba bean protein, casein, gelatin, *etc.*), composite type (protein/polysaccharides, protein/protein, ternary systems), and modified type (physical, Maillard reaction, cross-linking). Among various protein-based materials, whey protein, a known encapsulating agent for the targeted delivery of bioactive compounds, has attracted immense attention in the food industry (Khem et al., 2016). The amphiphilic characteristic of whey protein is contributed to its fast adsorption at the surface of the droplet and the formulation of a protective layer (Korma et al., 2018). In a previous study, the encapsulation efficiency of microcapsules fabricated with whey protein isolate/inulin reached up to 89.10% (Korma et al., 2018). Additionally, zein could be utilized to prepare the microcapsules for encapsulating the Zataria multiflora essential oil (Rasteh, Pirnia, Miri, & Sarani, 2024). Soy proteins exhibit excellent emulsifying ability, solubility, film-forming at the oil-water interface, and gelation properties (Yu et al., 2021). In recent years, there has been a growing interest in the utilization of pea proteins due to their low cost, low allergenicity, and potential health profits (Wang et al., 2022). As one of the most widely applied microencapsulation techniques, spray-drying has the potential to improve the bioavailability of ω-3 fatty acids and the stability of microcapsules (Bakry et al., 2015). Thus, the present study aimed to synthesize ω-3 MLCTs-based microcapsules with optimal characteristics, such as low free oil content, high solubility, and exceptional encapsulation efficiency, through spray-drying using soy, whey, or pea proteins as the wall materials.

Additionally, the effect of three different proteins on ω-3 MLCTs-based microcapsules was investigated to explore their contribution to the overall attributes and functionalities of the microcapsules. Overall, the ω-3 MLCTs-based microcapsules exhibited increased stability and encapsulation efficiency by reducing surface tension at the O/W interface. Moreover, the encapsulation method proved versatile, extending to low-viscosity oils such as citrus essential oil.

2. Materials and methods

2.1. Materials

Soy proteins (≥88% protein), whey proteins (≥90% protein), and pea proteins (≥86% protein) were purchased from Shandong Yuwang Industry Co., Ltd. Soy lecithin was provided by Donghai Grain and Oil Industry Co., Ltd. Other reagents were provided by Sigma-Alrich Chemicals (Shanghai, China).

2.2. Preparation of ω-3 MLCTs-based emulsions

The ω-3 MLCTs-based emulsions were prepared by the O/W template method with some modifications (Su et al., 2022). The ω-3 MLCTs used in the study were developed according to the previously reported method (Huang et al., 2020). Briefly, soy protein was dissolved in water to form a protein solution with a concentration of 7% *w/v*. Soy lecithin with 10 wt% was added to ω-3 MLCTs and mixed for 1 min using a high-speed disperser (T-18 digital ULTRA TURRAX, IKA) at a string speed of 12,000 r/min to form the emulsions. Then, 15 mL of the oil mixture was poured into a protein solution of 35 mL at an oil-to-protein mass ratio of 3:7. The suspensions obtained were stirred for 3 min using the high-speed disperser at the rate of 12,000 r/min to form an initial emulsion. Then, the initial emulsion was homogenized using high-pressure homogenization (80 Mpa, 8 min, and 25 °C) to attain an emulsion with uniform emulsification. Similarly, whey and pea proteins were incubated, and the MLCTs-based emulsions were developed.

2.3. Synthesis of microcapsules

Microencapsulation of MLCTs-based emulsions was achieved according to the previously reported method with minor modifications (Korma et al., 2018). The emulsions were incubated by spray-drying at a feed flow rate of 907 mL/h in a spray dryer (TriowinSD-1500, Shanghai, China), including a 120 kHz ultrasonic atomizing nozzle with two liquid channels. Nitrogen gas was used as the desiccant medium during spray-drying to keep the nozzle cool. Additionally, the contact between the liquid and gaseous phases was parallel current. The outlet and inlet temperatures of the spray dryer were set at 80 °C and 180 °C, respectively. The power obtained was collected for further analysis.

2.4. Droplet size properties

The average droplet size, size distribution, and polydispersity index (PDI) of the emulsions were measured using a dynamic light scattering instrument (Zatasizer Nano ZS90, Malvern Instruments Ltd., UK), according to the previously reported method with minor modifications (Guo et al., 2021). The emulsions were diluted by 100-fold with deionized water for shaking to form a uniform state and avoid the multiple light scattering effects. All measurements were carried out in the dispersion medium of deionized water using a refractive index of 1.33. The refractive and absorption indexes of the droplet were set as 1.46 and 0.1, respectively. The droplet size distribution was described using the PDI value of the droplet. All measurements were operated in triplicate at room temperature of 25 °C.

The particle size distributions of MLCTs microcapsules were determined by subjecting them to a drying process at 150 °C for 1 h, followed by ultrasonic dispersion in deionized water. Subsequently, ultrasonically treated HAMS microcapsules were subjected to analysis using the wet method with a refractive index of 1.548 (Tao & Xu, 2023).

2.5. Zeta-potential measurement

The electrical charges on the surface of the emulsion were determined using a Zetasizer Nano Z90 (Malvern Instruments Ltd., U·K) with a refractive index of 1.45 (Guo et al., 2021). The emulsions were diluted to a concentration of 0.01% (*w/v*) using a phosphate buffer solution of 10 mM at pH 7.0. After uniform mixing, 1 mL of the solution was poured into a sealed container and placed in a determination slot. All measurements were balanced at room temperature of 25 °C for 2 min.

2.6. CLSM

The microstructure and morphologies of the MLCTs-based emulsions were assessed using a confocal laser scanning microscope (LSM880, Carl Zeiss, Germany) (Hu et al., 2022). Each 1.0 mL of the protein-based sample was simply dyed with a 40 μL mixture of Nile Blue and Nile Red. Later, the stained sample between the cover glass and the slide was observed using a 40-power microscope with a pore size of 1.25 at 25 °C. The observation was operated at the excitation wavelengths of 633 nm and 480 nm, and the images were obtained at a scanning frequency of 100 Hz and fixed pixels of 1024 × 1024.

2.7. Desorption of adsorbed proteins at the interface

The proteins were desorbed according to the method of Lian et al. (Lian et al., 2022) with minor modifications. The fresh emulsions were centrifuged for 1 h (16,000 g, 4 °C) to separate the cream phase from the aspirated aqueous phase using a syringe. The aqueous phase was filtered through a 0.45 μm aqueous filter to remove the redundant lipid droplets and then freeze-dried to obtain the unabsorbed proteins at the interface. The cream phase was mixed with acetone at a ratio of 1:20 (*v*/v) and −20 °C, and then the mixture was stirred for 3 h. The lipid droplets on the surface of the precipitate were washed twice with cold acetone before removal. Finally, the precipitate was solubilized and freeze-dried to obtain the interfacial absorbed proteins.

2.8. Interfacial tension

The interfacial tension of the sample was determined according to the method of Lian et al. (Lian et al., 2022), with minor modifications. The emulsion interfacial state was continuously monitored *via* a DSA25 contact angle meter and the interfacial tension of the sample was calculated according to the Yang-Laplace capillary equation.

2.9. Rheology measurement

The steady-state rheology of different protein-based emulsions was assessed using a Modular Compact Rheometer (MCR302, Anton Paar, Austria). The shear rate or emulsion apparent viscosity was recorded at the range of 0.1–100 s^{-1}. The experiment was carried out at 25 °C, with a 0.5 mm slit distance and a 60 mm parallel plate clamp (Lian et al., 2022). The shear rate and apparent viscosity were fitted to the consistency coefficient and flow characteristic index using the Ostwald-Dewaele model. The formula was as follows:

$$\eta = K \times \gamma^{n-1} \tag{1}$$

where η is the apparent viscosity (Pa·s), K is the consistency coefficient (Pa·s^n), γ is the shear rate (s^{-1}), and n is the flow characteristic index ($n < 1$ indicates that the sample under investigation is a pseudoplastic non-Newtonian fluid, while $n = 1$ indicates that the sample is a Newtonian fluid).

2.10. Determination of surface oil and microencapsulation efficiency

The surface oil (SO) content and microencapsulation efficiency were determined according to the method described by Guo et al. (Guo et al., 2021), with some modifications. Briefly, 3.0 g of the microcapsule powder was mixed with 30 mL petroleum ether at a boiling range of 30–60 °C, followed by shaking and extracting for 2 min, and then filtered through a filter paper. The residues obtained were washed with 20 mL of petroleum ether and filtered using the same procedure. After filtering, the extracts were concentrated to remove petroleum ether and then dried until constant weight in an oven of 60 °C to obtain the microcapsule SO. The SO content of the microcapsule was calculated using the following Eq.:

$$A(\%) = \frac{m_2}{m_1} \times 100 \tag{2}$$

where: m_1 is the mass of microcapsule sample; m_2 represents the mass of SO of the microcapsules; A is the SO content of the microcapsules.

The total oil (TO) content of the microcapsules was determined by dispersing 3.0 g of microcapsule power in a Soxhlet extractor. Encapsulation Efficiency of the microcapsules refers to the oil encapsulated in the microcapsules to the TO content. Combined with the determination method of SO content, the microencapsulation efficiency was calculated using the following Eq.:

$$B(\%) = \frac{m_3 - m_2}{m_3} \times 100 \tag{3}$$

where m_3 represents the TO content of the microcapsules and B is the encapsulation efficiency of the microcapsules.

2.11. Solubility and moisture content analysis

The solubility index of different protein-based microcapsules was determined according to the method of Walker et al. (Walker Rebecca, McClements David, Decker Eric, & Cansu, 2017) with some modifications. Briefly, 3 g of protein-based microcapsule sample was added into 100 mL Milli-Q water and then stirred at 1000 r/min for maximum dissolving at room temperature of 25 °C. After mixing, the suspension was filtered through a quantitative filter paper. The filter paper obtained was dried until constant weight in an oven at 60 °C. The solubility index of the microcapsules was calculated using the following equation:

$$C(\%) = \left(1 - \frac{m_5 - m_4}{m_1}\right) \times 100 \tag{4}$$

where m_1 is the mass of the microcapsule sample; m_4 is the mass of the quantitative filter paper; m_5 is the mass of the filer paper and undissolved sample; C is the water solubility index of the microcapsules.

The moisture content of different microcapsules was determined according to the method of (Su et al., 2022) with minor modifications. The protein-based microcapsule samples were dried until constant weight in an oven at 105 °C in the bottle. The difference in the mass value between prior- and after-direct drying was calculated using the following Eq.:

$$D(\%) = \frac{m_6 - m_7}{m_6 - m_8} \times 100 \tag{5}$$

where m_6 represents the mass of the microcapsule samples and bottle, m_7 represents the mass of the microcapsule samples dried and bottle, m_8 represents the mass of the bottle used, and D is the moisture content of the microcapsules.

2.12. SEM

The morphology of different microcapsules was observed using SEM (JSM840, Jeol, Japan). The samples obtained were attached to an SEM stub with double-sided sticky tape. The sample and stub were coated with gold-palladium, and then the morphologies of three protein-based samples were photographed.

2.13. Storage stability

The storage stability of the spray-dried microcapsule was determined using the peroxide value (POV) during different incubation times. Briefly, the stability test was operated according to the method of Liu, with slight modifications (Liu, Zhang, Cui, Wang, & Wang, 2021). Liquid MLCTs and MLCTs-based microcapsule powers were sealed in oxygen-permeable plastic containers, which were then placed in an oven at 20 °C and 60 °C and stored for 10 weeks. The POV of the bulk MLCTs and

the microcapsules were determined every week. Prior to the determination of the peroxide index of the microcapsule power, the oil was extracted using a Soxhlet extractor. Data from samples were collected through titration using a sodium thiosulfate solution.

2.14. *In vitro* simulated digestion

The *in vitro* simulated digestion model was carried out according to the method described by Hu et al., with slight modifications (Hu, Dong, Hu, & Liu, 2023). Briefly, the MLCTs and MLCTs-based microcapsules were dissolved in diluted water, and then the pH of the solution obtained was adjusted to 2.0. Approximately 3.2 g of pepsin was added into 1 mL simulated gastric fluid, followed by addition of this fluid to the suspension. The measurement time points of simulated gastric digestion experiments were set as 5, 10, 20, 30, and 60 min during the 1-h digestion process. A part solution of the simulated fluid was taken out for ceasing enzymatic reaction, and the pH was adjusted to 6.5 by adding $NaHCO_3$ at a concentration of 1.5 mol/L. Another part of the solution was used for simulated intestinal digestion. Similarly, the pH value of this part fluid was adjusted to 7.5 using NaOH at a concentration of 0.2 mol/L. The measurement time point of stimulated intestinal digestion was set at 90 min and 120 min during the 1-h digestion process. After each stage of simulated conditions, the digesta was sampled to determine the amount of oil released from the microcapsules. During this digestion process, the pH of the solution was maintained at 7.5 using NaOH at a concentration of 0.2 mol/L, and NaOH consumption was recorded accurately.

The free fatty acid content in the *in vitro* digestion process was calculated using the following equation:

$$free\ fatty\ acids\ (\%) = \frac{V_{NaOH} \times C_{NaOH} \times M_{oil}}{2 \times W_{oil}} \times 100\% \quad (6)$$

where V_{NaOH} is the volume of NaOH utilized, C_{NaOH} is the concentration of NaOH, M_{oil} is the molecular weight of MLCT, W_{oil} is the total weight of MLCT in the microcapsule samples added.

2.15. Statistical analysis

Analytical determinations were carried out in duplicate for each replicate (three fresh replicates were obtained for each experimental condition). The results were calculated as mean ± standard deviations. All data were subjected to analysis of variance (ANOVA) assessed by Tukey's test using the SPSS 10.0 Statistical Software Program (SPSS Inc., Chicago, IL, USA) with a significance level of 5% ($p<0.05$).

3. Results and discussion

3.1. Droplet size analysis

Generally, the particle size and size distribution of emulsion droplets have a significant impact on the properties of microcapsules fabricated through the corresponding emulsion. Therefore, ascertaining the size distribution, average particle size, and PDI of different protein-based MLCTs emulsions is imperative to ensure the preparation of microcapsules with desirable characteristics. In this study, these parameters were determined and are shown in Fig. 1 and Table 1. The introduction of external mechanical forces, such as high homogenization pressure, has high significance for the successful formulation of optimal MLCTs emulsions due to the inability of various proteins and soy lecithin to independently form and stabilize emulsions.

As shown in Fig. 1, the droplet size of MLCTs emulsions fabricated with three different proteins had unimodal size distribution ranging from 100 to 600 nm. Generally, the droplets with unimodal size distributions are small with uniform size (Vidallon et al., 2022). Among the protein-based emulsions, the peak shape and peak area of the droplet

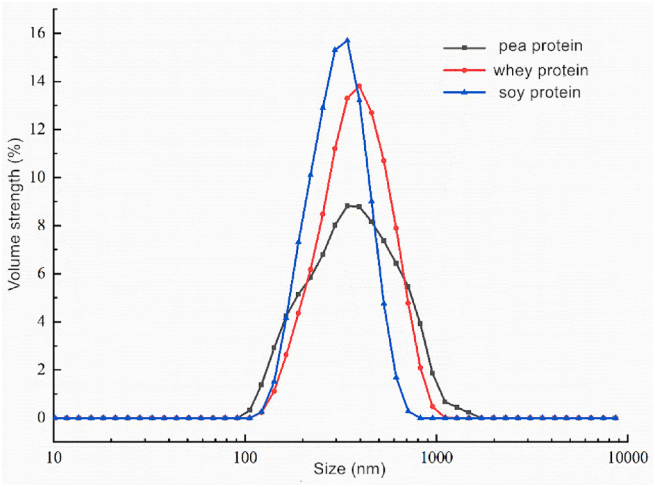

Fig. 1. Droplet size distribution of different protein-based MLCTs emulsions.

Table 1
The average particle size, PDI, and zeta-potential of different protein-based MLCTs emulsions.

Protein type	Particle size (nm)	PDI	ζ-potential(mV)
Whey protein	348.97 ± 10.26$^{b1)}$	0.26 ± 0.02^{b}	−31.28 ± 0.44^{b}
Soy protein	295.12 ± 11.65^{c}	0.24 ± 0.02^{b}	−32.65 ± 0.51^{a}
Pea protein	484.69 ± 13.54^{a}	0.35 ± 0.04^{a}	−28.17 ± 0.58^{c}

Data are expressed as mean ± SD (n = 3).
1) Values are means ± standard deviations of three replications. Different letters in the same column represent significant differences ($p < 0.05$).

size of soy protein-based MLCTs emulsions exhibited a narrow range compared to the size distribution of emulsion droplets fabricated with whey or pea proteins. This result demonstrated that the MLCTs-based emulsions fabricated with soy proteins had higher size uniformity following emulsification, with a more uniform particle distribution.

As shown in Table 1, the average particle size (295.12 ± 11.65 nm) of soy protein-based MLCTs emulsion was significantly smaller than that of whey or pea protein samples. This observation suggests that soy proteins play a crucial role in controlling the aggregation of ω-3 MLCTs droplets in the emulsion by forming an adsorption layer. This phenomenon contributes to the overall stability of the emulsions. Moreover, the PDI value of soy or whey protein samples was lower than that (0.35) of the pea protein samples (Table 1), which was consistent with the previous results of size distribution. Generally, a low PDI value of 0.3 and below is considered an acceptable carrier with a homogenous state in the drug delivery systems (Danaei et al., 2018). In this study, the low PDI value of soy protein (0.24) or whey protein (0.26) sample indicates that these two protein-based emulsion particles can be used in the carrier delivery field. Overall, all three proteins have the potential to form the oil-water interface mask with MLCTs through emulsification reaction due to their well emulsification characteristics. Additionally, the emulsions with unimodal size distribution and a narrow peak shape, small particle size, and low PDI value have a better uniform droplet distribution and stability (Primozic, Duchek, Nickerson, & Ghosh, 2017). Consequently, soy protein is more suitable for fabricating MLCTs emulsions compared with pea or whey protein.

Table S1 shows the cumulative particle size distributions of MLCTs microcapsules. Dx represents the cumulative particle size distribution percentage corresponding to a particle size reaching x%. D_{10}, D_{50}, and D_{90} represent the cumulative particle size distributions at 10%, 50%, and 90%, respectively. As shown in Table 1, the particle size distributions of MLCTs microcapsules with soy protein in D_{10}, D_{50}, and D_{90} were smaller than that of the whey or pea protein samples, which was

consistent with the SEM observations.

3.2. Zeta-potential analysis

In protein-based emulsions, the electrostatic repulsion force among protein-coated lipid droplets depends on the number of surface charges, which is detected by zeta-potential. Reflecting the stability of protein emulsion to some extent (Walker Rebecca et al., 2017). In this study, the zeta-potential of different MLCTs emulsions was detected, and the values are shown in Table 1. The zeta-potential values of all samples were negative, probably because the pH of the solution prepared was greater than the isoelectric point of the proteins used, resulting in many negative charges on the protein surface. Additionally, the absolute zeta-potential value of the emulsion fabricated with soy protein was significantly higher than that of the emulsion prepared with pea or whey proteins. The surface charges of the emulsions are mainly affected by the spatial conformation of proteins, the structural relaxation post-adsorption, and the rearrangement of proteins at the interface. Compared with the pea or whey protein samples, the soy protein samples exhibited greater relaxation and rearrangement at the MLCTs-aqueous phase interface, leading to the exposure of predominantly hydrophilic and hydrophobic groups of soy protein interior, which increased the number of charged amino acids on the interface proteins, the content of interface proteins, and the number of charges on the surface of droplet (Zhu, Xu, Liu, Xu, & Liu, 2019). Generally, the zeta-potential values of $> \pm$ 30 mV, $\pm$20–30 mV, and $\pm$ 10–20 mV have high stability, moderate stability, and relative stability for microcapsules, respectively (Su et al., 2022). The zeta potential values of soy or whey protein samples (−32.65 mV or − 31.28 mV) indicated their good stability and minimal dependence on the pH of different environments. The negative zeta-potential of soy lecithin aided in stabilizing the emulsion droplets during the emulsification process.

3.3. CLSM analysis

The images of the fabricated MLCTs emulsions were obtained using CLSM to explore the effect of different proteins on the microstructure of ω-3 MLCTs emulsions. Proteins were dyed with Nile blue, and oil droplets were dyed with Nile red. The CLSM images of the samples were used to clarify the interaction between the oil phase and aqueous phase at the interface of emulsion droplets. As shown in Fig. 2, the three protein-based MLCTs samples exhibited cores with red fluorescence and layer outsides with green fluorescence, which was consistent with the previous study, reporting a protein dyed green at the edge of the oil-

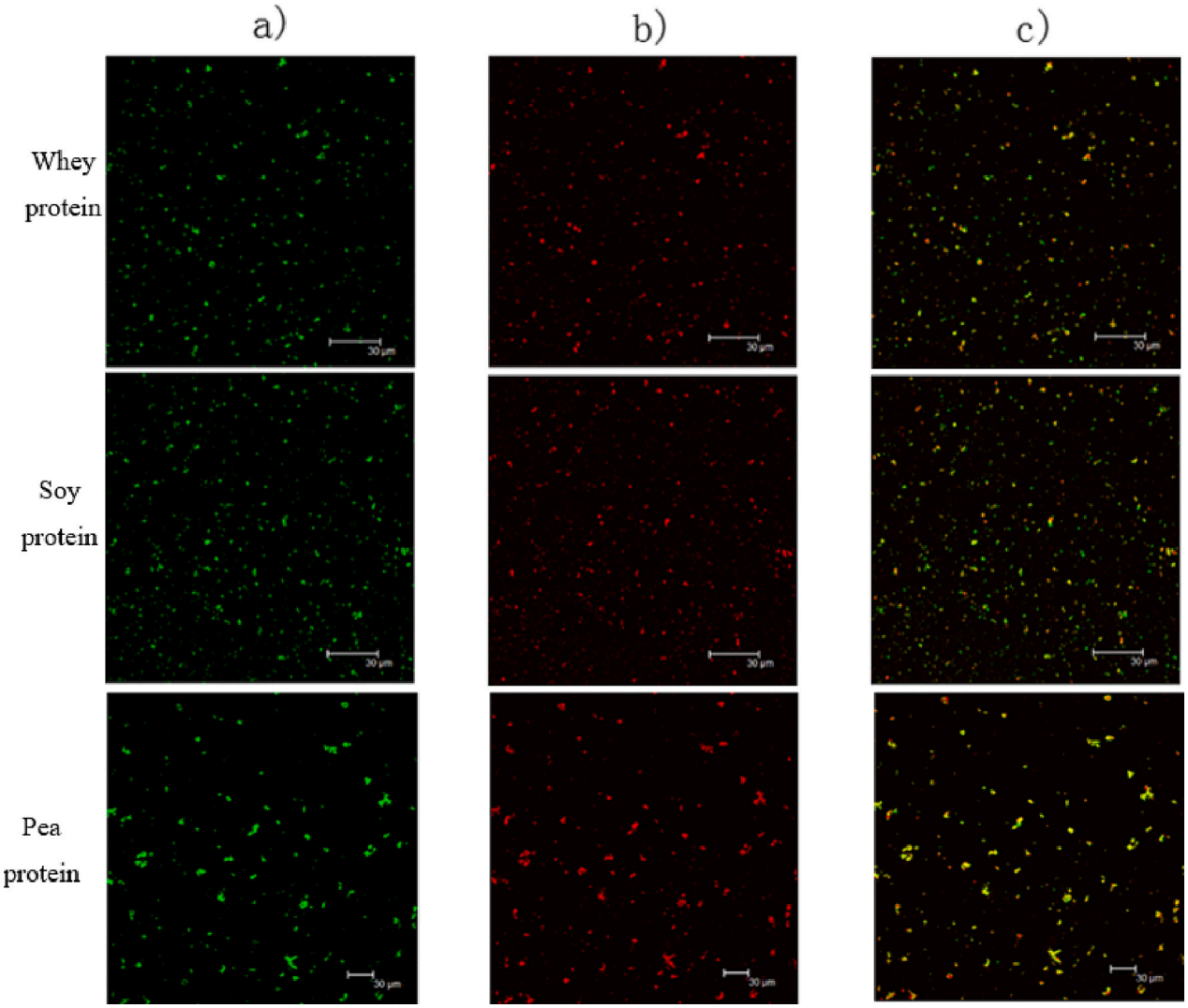

Fig. 2. CLSM images of whey protein, soy protein, or pea protein stabilized MLCTs emulsions. (a) protein phase containing Nile-blue dye (b) oil phase containing Nile-red dye (c) composite phase of protein and oil phase overlap. The scare bar in the image is 30 μm. (For interpretation of the references to colour in this figure legend, the reader is referred to the web version of this article.)

water droplets (Hu et al., 2022). The results indicated that three proteins were fully absorbed into the interface of the oil droplets, and the lipid phase was strongly coated into the emulsion droplets. Notably, the average droplet size distribution of the samples fabricated with soy protein was more uniform compared with the whey or pea protein samples. Additionally, the red image area of soy protein-based samples was comparatively smaller, suggesting a uniform distribution of the more oil phases in the soy protein matrixes. This result was consistent with the trend observed in Fig. 1. Compared with the whey or pea protein samples, the smaller size and uniform distribution of soy protein samples suggest a faster folding of soy protein onto the surface of oil droplets, thereby forming closer interfacial film with the protective on core materials. This phenomenon could be attributed to the higher protein absorption of soy protein (62.17%) at the interface of O/W, which prohibits aggregation of droplets, phase separation, or other unstable mechanisms of emulsion. Furthermore, the enhanced stability of MLCTs emulsion could be attributed to the increased amount of soy proteins absorbed at the interface of oil droplets, potentially leading to increased electrostatic repulsion between the emulsion droplets with negative charges from proteins. The absorbed proteins at the oil-water interface enhanced the stability of MLCTs emulsion droplets, facilitating the transformation of emulsion droplets into the protein-oil complexes (Hu et al., 2022). Overall, the outer protein layer surrounding the inner core material hinders oil droplets from aggregation and prevents particle deformation during the spray drying process.

3.4. Characterization of interface properties

In the food industry, proteins play a significant role in influencing the dispersibility and stability of emulsions, primarily due to their natural amphiphilic properties and the ability to reduce interfacial tension (Grasberger, Sunds, Sanggaard, Hammershøj, & Corredig, 2022). In this study, the interfacial protein concentration, interfacial tension, and apparent viscosity of various protein-based samples were measured to investigate the effect of different protein types on the interface of ω-3 MLCTs emulsions, and the results are presented in Table 2 and Fig. 3. As shown in Table 2, the soy protein-based emulsion showed a higher protein absorption of 62.17% at the O/W interface compared with the whey or pea protein samples. The adsorption of protein to the interface can be generally distilled to these steps: (1) the diffusion of protein between oil droplets and liquid phase; (2) the position of protein on the oil-water interface; (3) the formation of interfacial protein film based on the rearrangement or cross-link interaction of protein on the droplets surface; (4) the saturate adsorption of protein on the oil-water interface (Beverung, Radke, & Blanch, 1999). Furthermore, the physicochemical properties of different protein-based droplets influence protein adsorption at the interface (Grasberger et al., 2022). These results demonstrated that the smaller particle size, greater electrostatic repulsion between droplets, easier film-forming ability at the interface, and higher interface flexibility of soy protein samples contributed to their more rapid adsorption at the interface of the droplets compared with the whey or pea protein samples. This finding indicated that soy protein had a stronger affinity to the droplet of ω-3 MLCTs emulsion than the whey and pea protein samples. After adsorption, proteins tend to maintain

Table 2
The interfacial protein content and interfacial tension of different protein-based MLCTs emulsions.

Protein type	Interfacial protein content (%)	Interfacial tension (mN/m)
Whey protein	58.65 ± 1.24[b1)]	24.29 ± 0.81[b]
Soy protein	62.17 ± 0.88[a]	21.36 ± 0.65[c]
Pea protein	49.84 ± 1.16[c]	29.14 ± 1.12[a]

Data are expressed as mean ± SD ($n = 3$).
1) Values are means ± standard deviations of three replications. Different letters in the same column represent significant differences ($p < 0.05$).

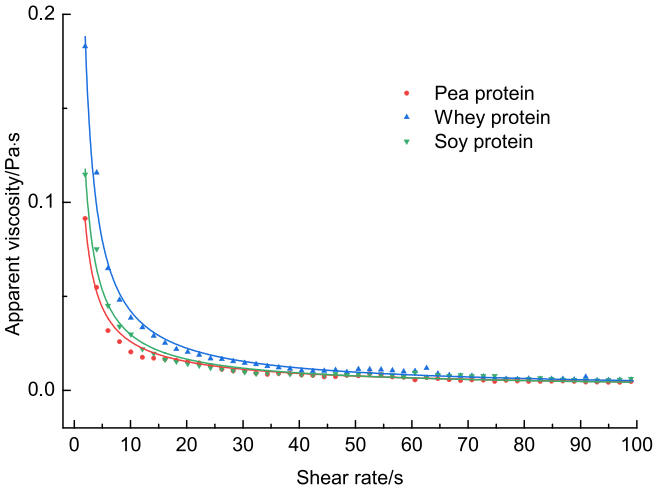

Fig. 3. The apparent viscosity of different protein-based MLCTs microcapsules at 25 °C.

their natural conformation at the interface, with more flexible proteins undergoing rapid rearrangement (Shen et al., 2023). Moreover, native whey and pea proteins predominantly possess globular structures, consisting mainly of globular β–lactoglobulin and globulins, respectively (D'Alessio et al., 2023). Herein, the surface tension of ω-3 MLCTs emulsions was notably lower than 30 mN/m (Korma et al., 2018), suggesting higher surface activity at the air-water interface.

The soy protein samples demonstrated more rapid adsorption at the emulsion interface and contributed to a faster decrease in interfacial tension. As shown in Table 2, the soy protein samples showed a lower interfacial tension of 21.36 mN/m compared with the whey or pea protein samples. The lower interfacial tension of soy protein indicated more flexible stretching and sustained adsorption at the O/W interface, which was consistent with another finding of CLSM. This result confirms that soy protein is more suitable for adsorbing at the interface of O/W and improving the stability of ω-3 MLCTs-based emulsions. Based on the comparison of tension, it was speculated that the soy protein emulsions could increase the adsorption efficiency.

3.5. Rheological properties analysis

The steady-state rheological behavior directly reflects the changes in the dispersive motion speed, providing insights into the microstructural mechanical properties, which are essential parameters (Lian et al., 2022). Fig. 3 and Table 3 illustrate the apparent viscosity of different protein-based samples ranging from 1 to 100 s^{-1} and the steady shear rheological parameters based on the Ostwald-Dewaele model, respectively. At the initial state of the steady-state rheology test, the apparent viscosity of the whey protein sample was slightly higher than that of soy and pea protein samples, which might be ascribed to the differences in protein adsorption at the interface. However, as the shear rate increased to 100 s^{-1}, all three protein samples exhibited low apparent viscosity

Table 3
The steady-state rheology indicators of MLCTs emulsions stabilized by different protein.

Protein type	Consistency coefficient ($Pa·s^n$)	Flow characteristic index/n	Correlation coefficient/R^2
Whey protein	0.213	0.107	0.99
Soy protein	0.347	0.088	0.99
Pea protein	0.163	0.113	0.98

with no significant differences. Fig. 3 exhibits a typical shear-thinning behavior for all protein-based samples, indicating that the MLCTs emulsions fabricated using different proteins are non-Newtonian fluids. This behavior can be attributed to the gradual dispersion of the MLCTs emulsion network structure with increased shear rate (Feng et al., 2022). The shear-thinning behavior of MLCTs emulsions is beneficial for preventing droplets from creaming and facilitating the flow of food-grade emulsion during the microencapsulation process. Additionally, the viscosity curve shows a good correlation with the Ostwald-Dewaele model, with a correlation coefficient (R^2) close to 1.0 (Table 3). Notably, the flow characteristic index (n) was significantly <1.0 (0.088–0.113), confirming the non-Newtonian shear-thinning performance of the emulsions. This result could be attributed to the fracture and distraction of the droplets or emulsion network (Horozov, Binks, & Gottschalk-Gaudig, 2007). Among all samples, the soy protein samples showed the highest K value, indicating that the soy protein-based emulsion has excellent stability. These observations suggest that the addition of soy protein enhances the stability of ω-3 MLCTs emulsions. Furthermore, the viscosity of ω-3 MLCTs emulsion was lower, reaching below 0.2 Pas. This characteristic is conducive to atomization during the spray-drying process, distinguishing it from the reported study on MLCTs (Korma et al., 2018). This reduced viscosity could enhance the feasibility of spray-drying, highlighting the potential applicability and efficiency of ω-3 MLCTs emulsion in contrast to previous research (Korma et al., 2018).

3.6. Physicochemical properties of microcapsules

The SO content, encapsulation efficiency, solubility, and moisture content of microcapsules are important indicators for further application in the food industry (Jamshidi, Cao, Xiao, & Simal-Gándara, 2020). After spray-drying of protein-based MLCTs emulsions, the physicochemical characteristics of the obtained MLCTs microcapsules were examined, and the results are shown in Table S2. As shown in Table S2, the MLCTs microcapsules fabricated with soy protein had a lower SO content of 0.75% and a higher encapsulation efficiency of 94.56%, suggesting better protection of soy protein on core MLCTs and making it less prone to oxidation when exposed to external conditions. This might be attributed to the good encapsulation efficiency of soy protein, facilitated by faster adsorption, stronger electrostatic repulsion, and a larger interfacial area of the small-sized soy protein samples onto the interface of droplets during emulsification. Additionally, the smooth and complete spherical structure with a thick outer layer of soy protein microcapsules during drying contributed to their enhanced protection. In contrast to the antecedent study on MLCTs (Korma et al., 2018), this study revealed a substantial reduction in the SO content within the microcapsules. The observed decrease in SO content underscores the potential impact of formulation nuances on the composition of microcapsules. The decreased SO content in all samples was consistent with the previous study results of Jamshidi et al., suggesting that a lower SO content in the surface or inner part of microcapsules makes them less prone to oxidation, enhancing the dispersibility and wettability of their efficiency (Jamshidi et al., 2020). They also found that the SO content in the spray-dried microcapsules, consisting of different polysaccharides or proteins, was much dependent on the wall material, core/wall ratio, and manufacturing operations (Jamshidi et al., 2020). Herein, under the same oil-water ratio and treatment conditions, soy protein maintained the stability of microcapsules better, especially in terms of the differences in SO content and encapsulation efficiency. Furthermore, the encapsulation efficiency of MLCTs microcapsules exhibited a noteworthy elevation compared to that reported in a previous investigation (89.10%) (Korma et al., 2018).

As shown in Table S2, the soy, whey, or pea protein-based microcapsules showed no significant differences in their solubility, which is beneficial for further applications of microcapsules. Among these samples, the solubility of soy protein microcapsules was the highest at 96.12%, due to the lower SO content loading of the powder (Guo, Fan, Zhou, & Li, 2023). Compared with the solubility of other studies on protein-based microcapsules (Guo et al., 2023), the values of the three protein-based microcapsules in this study were higher, above 92%, indicating that the hydrophobic groups of soy, whey, or pea proteins are closely associated with the fat-soluble core. Additionally, there were no remarkable differences in the moisture content among the three protein samples. All samples showed low moisture values of about 4.0%, which is commonly considered a desirable characteristic of dried power used in the food industry (Yildiz, Ding, Gaur, Andrade, & Feng, 2018). The low moisture content of microcapsules is conducive to enhancing the storage stability of MLCTs microcapsules. The alteration in the structural state of the wall material, transitioning from a glassy state to an amorphous state, might be attributed to the high moisture level within the system, leading to the release and degradation of the core component during the storage period. The slight difference in the moisture content among the samples might be attributed to the diffusion coefficients of water through different protein wall materials or the difference in affinity of proteins to water.

3.7. Morphology of proteins microcapsules

The microstructures of different protein-based microcapsules after spray-drying were obtained by SEM, and the results are shown in Fig. 4. Generally, the size of microcapsules obtained through spray-drying treatment ranges from 1 to 50 μm (Nesterenko, Alric, Silvestre, & Durrieu, 2013). Herein, a high dispersibility of different protein-based microcapsules was observed due to the formation of droplets with different sizes during the emulsification process. Among all samples, the size of most microcapsules ranged from 1.0 to 9.5 μm, which was consistent with the result of fish oil microcapsules stabilized by whey, soy, and potato proteins (Hadnađev et al., 2023) and the predicted result of Fig. 1. As for the whey and pea protein-based samples, some wrinkles and dents with an irregular state were observed on the surface of the microcapsules. This might be attributed to the formation of an uneven film on the microcapsule surfaces due to the dynamical dehydration of liquid drops during spray-drying. Similar characters were also reported by Hadanadev et al., who fabricated fish oil microcapsules stabilized by whey protein (Hadnađev et al., 2023). Notably, these two protein-based samples exhibited a central hollow structural characteristic, probably due to the rapid expansion of the particles at the final stage of spray drying (Su et al., 2022). After the addition of soy protein to the wall material, the MLCTs microcapsules exhibited a nearly spherical, smooth surface, and regular shape (Fig. 4B). This could be attributed to the smaller particle size of the fed emulsion, higher elasticity, and higher solution viscosity of soy protein (Hadnađev et al., 2023). This smooth surface of soy protein-based microcapsules could provide good protection for encapsulated oil, maintain low permeability, and reduce the intervention of external factors such as oxygen and heat during storage (Su et al., 2022).

3.8. Storage stability of microcapsules

High storage stability can significantly maintain the quality of MLCTs microcapsules in the food industry. Typically, the α-linolenic acid in MLCTs is sensitive to heat, light, oxygen, and metal ions, making it prone to oxidation. Oxidation products of oils may not be beneficial to the human body. As one of the most crucial factors for preserving heat-sensitive materials, including flavors, nutrients, and microorganisms, storage temperature is conducive to evaluating the stability of ω-3 MLCTs microcapsules during storage (Hadnađev et al., 2023). In this study, the oxidative stability of protein-based microcapsules during storage was studied, and the results are shown in Fig. 5. With a rapid increase in the speed of oil oxidation, the ω-3 MLCTs became highly oxidable. After ten weeks of storage at 20 °C or 60 °C, the POV content of the control samples increased from 0.4 and 0.6 mmol/kg initially to 15.18 and 49.36 mmol/kg, respectively. However, these protein-based

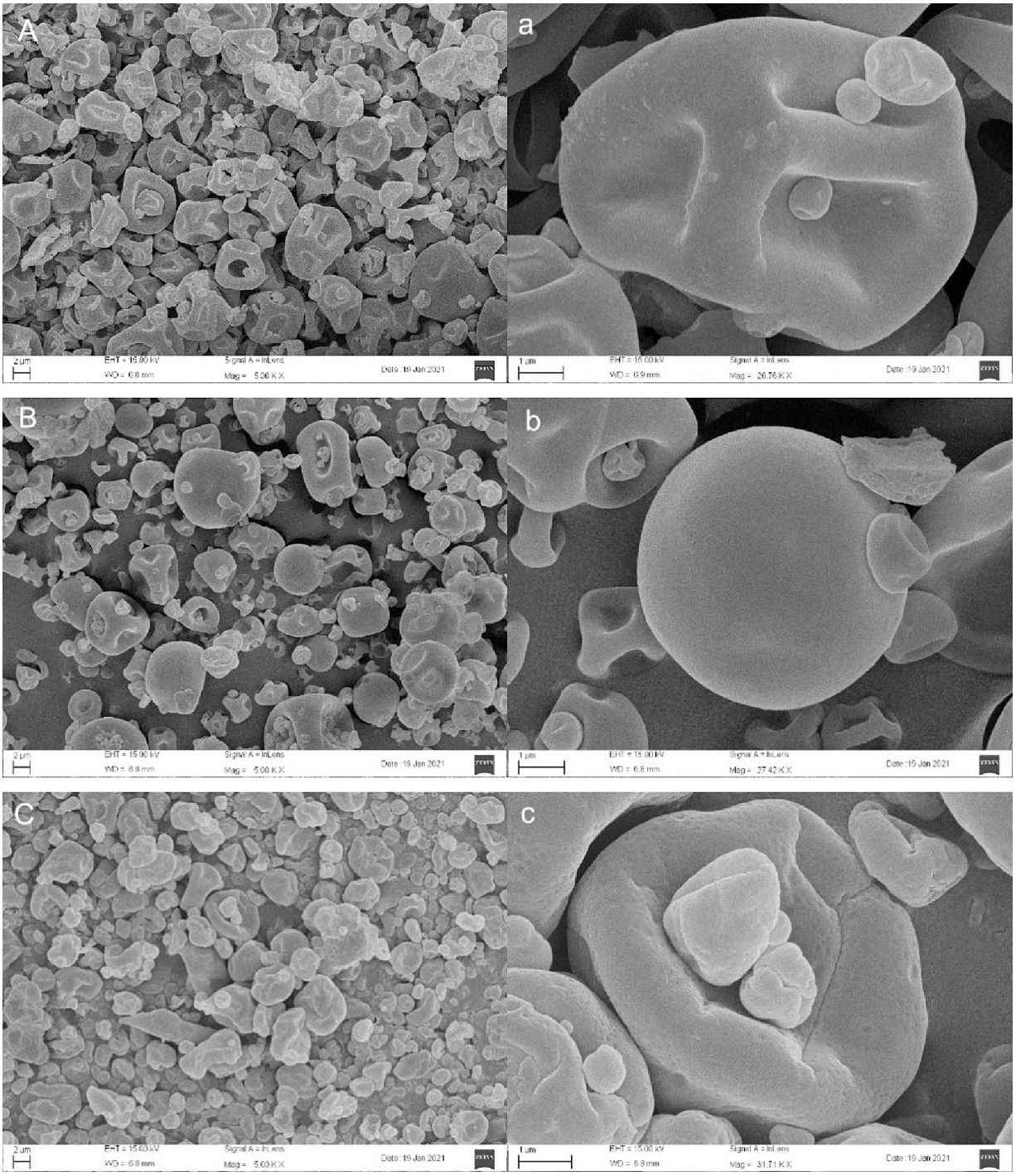

Fig. 4. The microstructures of whey protein (A), soy protein (B), or pea protein (C) MLCTs microcapsules at magnification of × 5000 and the morphology of the microcapsule fabricated with the whey protein (a), soy protein (b), or pea protein (c) observed by SEM at high magnification.

microcapsule powers exhibited lower POV at different incubation temperatures compared with the samples without treatment. This demonstrated that the microencapsulation of proteins significantly enhanced the antioxidant stability of ω-3 MLCTs. After being stored at 20 °C or 60 °C for 10 weeks, the POV of the soy protein sample reached the lowest at 0.77 or 5.13 mmol/kg. This phenomenon indicated that soy protein had a better protective action on easily oxidizable fatty acids of MLCTs compared with whey or pea proteins. The superior antioxidant stability might be attributed to the oxygen barrier effect of the soy protein microcapsules in the form of strong surface films at the interface of oil droplets, which could effectively separate the direct contact between core oil and external environments such as light and heat. The result was consistent with the findings of Fig. 1&3 and Table 1. The smaller particle size and spherical shape of soy protein samples could prevent the coalescence of droplets during the spray-drying process and make the microcapsules more complete, leading to an enhanced oxidation stability of MLCTs microcapsules through soy protein treatment. Furthermore, a positive correlation was observed between the SO content and POV due to the direct contact between exposed oil and oxygen (Castro, Cespedes, Carballo, Bergenstahl, & Tornberg, 2013). The lowest SO content of soy protein samples among the three protein samples contributes to verifying their low POV in Fig. 5. This phenomenon could also be explained

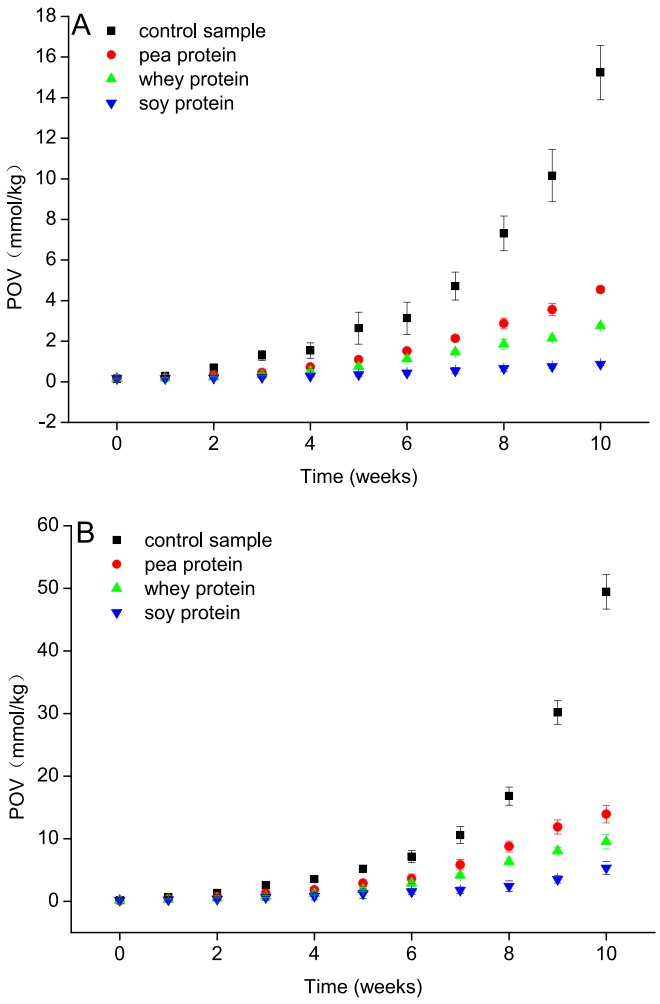

Fig. 5. The storage stability of different protein-based MLCTs microcapsules and control samples at 20 °C (A) and 60 °C (B) for 10 weeks.

by the treatment of high temperature and pressure, leading to the stretch of the protein structure and providing more hydrophobic amino acids to bind SO (Castro et al., 2013).

3.9. In vitro simulation of gastrointestinal digestion

The release profiles of different protein-based MLCTs microcapsules and MLCTs under consecutive simulated gastric and intestinal digestion are presented in Fig. S1. A slow release of MLCTs without treatment occurred during gastric and intestinal digestion, and the release rate increased from 68.23% initially to 97.49%, which was significantly higher than the microcapsule samples. After microencapsulation, the release rate of pea protein-based microcapsules was higher than that of the whey or soy protein samples during the first 60 min of gastric digestion. This phenomenon might be ascribed to the dents and cracks on the microcapsule surface caused by the dehydration shrinkage of microcapsules during the spray-drying process, thus making the pea protein microcapsules more prone to exposure to gastric juice than other types of protein-based samples. This finding was consistent with the SEM results in Fig. 4. Additionally, a low release of whey protein samples was observed (Fig. S1), which was consistent with the findings of Mohammadian, reporting whey protein microgels with slow release during simulated gastrointestinal digestion (Mohammadian, Salami, Momen, Alavi, & Emam-Djomeh, 2019). Among these samples, the release rate of soy protein samples during the simulation phase was the lowest, which might be due to the spherical shape of soy protein microcapsule after spray-drying, the well-buffering effect of soy protein consisting of amino groups, and carboxyl groups (Liu et al., 2021), and the strong intermolecular forces between soy protein and MLCTs droplets.

4. Conclusion

In this study, novel ω-3 MLCTs microcapsules were fabricated using soy, whey, or pea proteins in conjunction with a spray-dried treatment. Additionally, the impact of various proteins on the properties of these SL microcapsules was investigated through a series of assessments. The ω-3 MLCTs emulsions fabricated with soy protein as the wall material showed the most ideal state, with a particle size of 295.12 nm, zeta-potential of −32.65 mV, and PDI value of 0.24. Additionally, the emulsion characteristics of the soy protein-based samples were conducive to reserving more protein and maintaining less interfacial tension at the interface of droplets. These emulsion properties also contributed to the formation of complete and spherical microcapsules after spray-drying treatment. Furthermore, the soy protein-based microcapsules exhibited lower SO content and higher encapsulation efficiency. Consequently, these soy protein-based microcapsules demonstrated a more intensive protective effect on core actives compared with the whey or pea protein samples. Moreover, these proteins demonstrated an effective enhancement in the storage stability of ω-3 MLCTs microcapsules, serving as efficient encapsulating agents. This improvement is conducive to the vivo application of ω-3 MLCTs microcapsules. Overall, this research presents a pivotal advancement with far-reaching implications for the utilization of ω-3 MLCTs microcapsules formulated from diverse proteins across various industries, paving the way for extensive possibilities in the food, biomedical, and cosmetic sectors.

CRediT authorship contribution statement

Zhen Yang: Writing – original draft, Methodology, Investigation, Formal analysis, Data curation, Conceptualization. **Yujie Guo:** Supervision, Writing – review & editing. **Chili Zeng:** Methodology, Formal analysis, Data curation. **Fuwei Sun:** Supervision, Software, Formal analysis. **Zhongjiang Wang:** Supervision, Data curation. **Weimin Zhang:** Methodology, Formal analysis. **Tian Tian:** Formal analysis, Data curation. **Lingyue Shan:** Software, Formal analysis. **Yunxiang Zeng:** Writing – review & editing. **Zhaoxian Huang:** Writing – review & editing, Methodology, Investigation, Funding acquisition, Formal analysis, Conceptualization. **Lianzhou Jiang:** Writing – review & editing, Investigation, Funding acquisition, Formal analysis, Conceptualization.

Declaration of competing interest

The authors declare that they have no known competing financial interests or personal relationships that could have appeared to influence the work reported in this paper.

Data availability

Data will be made available on request.

Acknowledgements

This research was supported by the National Natural Science Foundation of China (No: 32360589, 32230082, and 32260609), International Science & Technology Cooperation Program of Hainan Province (No: GHYF2023006), Hainan Provincial Natural Science Foundation of China (No: 322QN245), and Hainan University Research Start-up Fund (No: KYQD(ZR)-22011), The China Postdoctoral Science Foundation (No: 2023M732131), The Research Project of the Collaborative Innovation Center of Hainan University (No: XTCX2022NYC20), Hainan Province Science and Technology Special Fund (No:

ZDYF2024XDNY170).

Appendix A. Supplementary data

Supplementary data to this article can be found online at https://doi.org/10.1016/j.fochx.2024.101363.

References

Bakry, A. M., Abbas, S., Ali, B., Majeed, H., Abouelwafa, M., Mousa, A., & Liang, L. (2015). Microencapsulation of oils: A comprehensive review of benefits, techniques, and applications. *Comprehensive Reviews in Food Science and Food Safety, 15*, 143–182. https://doi.org/10.1111/1541-4337.12179

Beverung, C. J., Radke, C. J., & Blanch, H. W. (1999). Protein adsorption at the oil/water interface: Characterization of adsorption kinetics by dynamic interfacial tension measurements. *Biophysical Chemistry, 81*(1), 59–80. https://doi.org/10.1016/S0301-4622(99)00082-4

Castro, A., Cespedes, G., Carballo, S., Bergenstahl, B., & Tornberg, E. (2013). Dietary fiber, fructooligosaccharides, and physicochemical properties of homogenized aqueous suspensions of yacon (Smallanthus sonchifolius). *Food Research International, 50*(1), 392–400. https://doi.org/10.1016/j.foodres.2012.10.048

Cheng, X., Jiang, C., Jin, J., Jin, Q., Akoh, C. C., Wei, W., & Wang, X. (2024). Medium- and long-chain triacylglycerol: Preparation, health benefits, and food utilization. *Annual review of food science and technology., 15*(1). https://doi.org/10.1146/annurev-food-072023-034539

D'Alessio, G., Flamminii, F., Faieta, M., Prete, R., di Michele, A., Pittia, P., & Di Mattia, C. D. (2023). High pressure homogenization to boost the technological functionality of native pea proteins. *Current Research in Food Science, 6*, Article 100499. https://doi.org/10.1016/j.crfs.2023.100499

Danaei, M., Dehghankhold, M., Ataei, S., Hasanzadeh, D. F., Javanmard, R., Dokhani, A., … Mozafari, M. (2018). Impact of particle size and polydispersity index on the clinical applications of lipidic nanocarrier systems. *Pharmaceutics, 10*(2), 57. https://doi.org/10.3390/pharmaceutics10020057

Du, Y. X., Chen, S. N., Zhu, H. L., Niu, X., Li, J., Fan, Y. W., & Deng, Z. Y. (2020). Consumption of Interesterified medium- and long-chain Triacylglycerols improves lipid metabolism and reduces inflammation in high-fat diet-induced obese rats. *Journal of Agricultural and Food Chemistry, 68*(31), 8255–8262. https://doi.org/10.1021/acs.jafc.0c03103

Feng, X., Dai, H., Fu, Y., Yu, Y., Zhu, H., Wang, H., Ma, L., & Zhang, Y. (2022). Regulation mechanism of nanocellulose with different morphologies on the properties of low-oil gelatin emulsions: Interfacial adsorption or network formation? *Food Hydrocolloids, 133*, Article 107960. https://doi.org/10.1016/j.foodhyd.2022.107960

Gharsallaoui, A., Roudaut, G. L., Chambin, O., Voilley, A., & Saurel, R. (2007). Applications of spray-drying in microencapsulation of food ingredients: An overview. *Food Research International, 40*(9), 1107–1121. https://doi.org/10.1016/j.foodres.2007.07.004

Grasberger, K., Sunds, A. V., Sanggaard, K. W., Hammershøj, M., & Corredig, M. (2022). Behavior of mixed pea-whey protein at interfaces and in bulk oil-in-water emulsions. *Innovative Food Science & Emerging Technologies, 81*, Article 103136. https://doi.org/10.1016/j.ifset.2022.103136

Guo, L., Fan, L., Zhou, Y., & Li, J. (2023). Constitution and reconstitution of microcapsules with high diacylglycerol oil loading capacity based on whey protein isolate / octenyl succinic anhydride starch/ inulin matrix. *International Journal of Biological Macromolecules, 242*, Article 124667. https://doi.org/10.1016/j.ijbiomac.2023.124667

Guo, Z., Huang, Z., Guo, Y., Li, B., Yu, W., Zhou, L., … Wang, Z. (2021). Effects of high-pressure homogenization on structural and emulsifying properties of thermally soluble aggregated kidney bean (Phaseolus vulgaris L.) proteins. *Food Hydrocolloids, 119*, Article 106385. https://doi.org/10.1016/j.foodhyd.2021.106835

Hadnađev, M., Kalić, M., Krstonošić, V., Jovanović-Lješković, N., Erceg, T., Škrobot, D., & Dapčević-Hadnađev, T. (2023). Fortification of chocolate with microencapsulated fish oil: Effect of protein wall material on physicochemical properties of microcapsules and chocolate matrix. *Food Chemistry: X, 17*, Article 100583. https://doi.org/10.1016/j.fochx.2023.100583

Horozov, T. S., Binks, B. P., & Gottschalk-Gaudig, T. (2007). Effect of electrolyte in silicone oil-in-water emulsions stabilised by fumed silica particles. *Physical Chemistry Chemical Physics, 9*(48), 6398–6404. https://doi.org/10.1039/b709807n

Hu, R., Dong, D., Hu, J.-L., & Liu, H. (2023). Improved viability of probiotics encapsulated in soybean protein isolate matrix microcapsules by coacervation and cross-linking modification. *Food Hydrocolloids, 138*, Article 108457. https://doi.org/10.1016/j.foodhyd.2023.108457

Hu, Y., Yang, S., Zhang, Y., Shi, L., Ren, Z., Hao, G., & Weng, W. (2022). Effects of microfluidization cycles on physicochemical properties of soy protein isolate-soy oil emulsion films. *Food Hydrocolloids, 130*, Article 107684. https://doi.org/10.1016/j.foodhyd.2022.107684

Huang, Z., Cao, Z., Guo, Z., Chen, L., Wang, Z., Sui, X., & Jiang, L. (2020). Lipase catalysis of alpha-linolenic acid-rich medium- and long-chain triacylglycerols from perilla oil and medium-chain triacylglycerols with reduced by-products. *Journal of the Science of Food and Agriculture, 100*(12), 4565–4574. https://doi.org/10.1002/jsfa.10515

Jamshidi, A., Cao, H., Xiao, J., & Simal-Gándara, J. (2020). Advantages of techniques to fortify food products with the benefits of fish oil. *Food Research International, 137*, Article 109353. https://doi.org/10.1016/j.foodres.2020.109353

Khem, S., Bansal, V., Small, D. M., & May, B. K. (2016). Comparative influence of pH and heat on whey protein isolate in protecting lactobacillus plantarum A17 during spray drying. *Food Hydrocolloids, 54*(mar.pt.A), 162–169. https://doi.org/10.1016/j.foodhyd.2015.09.029

Korma, S. A., Wei, W., Ali, A. H., Abed, S. M., & Wang, X. (2018). Spray-dried novel structured lipids enriched with medium-and long-chain triacylglycerols encapsulated with different wall materials: Characterization and stability. *Food Research International, 116*, 538–547. https://doi.org/10.1016/j.foodres.2018.08.071

Lai, Y., Li, D., Liu, T., Wan, C., Zhang, Y., Zhang, Y., & Zheng, M. (2023). Preparation of functional oils rich in diverse medium and long-chain triacylglycerols based on a broadly applicable solvent-free enzymatic strategy. *Food research international (Ottawa, Ont.), 164*, Article 112338. https://doi.org/10.1016/j.foodres.2022.112338

Lee, Y. Y., Tang, T. K., Chan, E. S., Phuah, E. T., & Tan, J. S. (2021). Medium chain triglyceride and medium-and long chain triglyceride: Metabolism, production, health impacts and its applications – A review. *Critical Reviews in Food Science and Nutrition, 62*(3), 1–17. https://doi.org/10.1080/10408398.2021.1873729

Li, W. Z., & Hui. (2021). Synthesis of medium and long-chain triacylglycerols by enzymatic acidolysis of algal oil and lauric acid. *LWT-Food Science & Technology, 136*(Pta1), Article 110309. https://doi.org/10.1016/j.lwt.2020.110309

Lian, Z., Yang, S., Cheng, L., Liao, P.-B., Dai, S., Tong, X., Tian, T., Jiang, L., & Wang, H. (2022). Emulsifying properties and oil–water interface properties of succinylated soy protein isolate: Affected by conformational flexibility of the interfacial protein. *Food Hydrocolloids, 136*, Article 108224. https://doi.org/10.1016/j.foodhyd.2022.108224

Liu, Y., Zhang, C., Cui, B., Wang, M., & Wang, Y. (2021). Carotenoid-enriched oil preparation and stability analysis during storage: Influence of oils' chain length and fatty acid saturation. *LWT- Food Science and Technology, 151*(4), Article 112163. https://doi.org/10.1016/j.lwt.2021.112163

Mohammadian, M., Salami, M., Momen, S., Alavi, F., & Emam-Djomeh, Z. (2019). Fabrication of curcumin-loaded whey protein microgels: Structural properties, antioxidant activity, and in vitro release behavior. *LWT, 103*, 94–100. https://doi.org/10.1016/j.lwt.2018.12.076

Nesterenko, A., Alric, I., Silvestre, F. O., & Durrieu, V. (2013). Vegetable proteins in microencapsulation: A review of recent interventions and their effectiveness. *Industrial Crops and Products, 42*(1), 469–479. https://doi.org/10.1016/j.indcrop.2012.06.035

Primozic, M., Duchek, A., Nickerson, M., & Ghosh, S. (2017). Effect of lentil proteins isolate concentration on the formation, stability and rheological behavior of oil-in-water nanoemulsions. *Food Chemistry, 237*(dec.15), 65–74. https://doi.org/10.1016/j.foodchem.2017.05.079

Ramakrishnan, S., Ferrando, M., Aceña-Muñoz, L., Mestres, M., Lamo-Castellví, S. D., & Güell, C. (2013). Influence of emulsification technique and wall composition on physicochemical properties and oxidative stability of fish oil microcapsules produced by spray drying. *Food and Bioprocess Technology, 7*, 1959–1972. https://doi.org/10.1007/s11947-013-1187-4

Rasteh, I., Pirnia, M., Miri, M. A., & Sarani, S. (2024). Encapsulation of Zataria multiflora essential oil in electrosprayed zein microcapsules: Characterization and antimicrobial properties. *Industrial Crops and Products, 208*, Article 117794. https://doi.org/10.1016/j.indcrop.2023.117794

Shen, Q., Li, J., Shen, X., Zhu, X., Dai, J., Tang, C., Song, R., Li, B., & Chen, Y. (2023). Linear and nonlinear interface rheological behaviors and structural properties of pea protein (vicilin, legumin, albumin). *Food Hydrocolloids, 139*, Article 108500. https://doi.org/10.1016/j.foodhyd.2023.108500

Su, X., Xu, Y., Xu, Z., Hurley, K., Feng, Y., & Yin, Y. (2022). Encapsulation of hop (Humulus lupulus L.) essential oil for controlled release in the non-alcoholic beverage application. *Food Hydrocolloids, 134*, Article 108039. https://doi.org/10.1016/j.foodhyd.2022.108039

Tao, M., & Xu, T. (2023). Development and properties of bio-based rice oil microcapsule and its dispersibility in emulsified asphalt. *Journal of Industrial and Engineering Chemistry, 131*, 503–513. https://doi.org/10.1016/j.jiec.2023.10.054

Vega, C., Kim, E.-H.-J., Chen, X. D., & Roos, Y. H. (2005). Solid-state characterization of spray-dried ice cream mixes. *Colloids and Surfaces B: Biointerfaces, 45*(2), 66–75. https://doi.org/10.1016/j.colsurfb.2005.07.009

Vidallon, M. L. P., Salimova, E., Crawford, S. A., Teo, B. M., Tabor, R. F., & Bishop, A. I. (2022). Enhanced photoacoustic imaging in tissue-mimicking phantoms using polydopamine-shelled perfluorocarbon emulsion droplets. *Ultrasonics Sonochemistry, 86*, Article 106041. https://doi.org/10.1016/j.ultsonch.2022.106041

Walker Rebecca, M., McClements David, J., Decker Eric, A., & Cansu, E. (2017). Improvements in the formation and stability of fish oil-in-water nanoemulsions using carrier oils: MCT, thyme oil, & lemon oil. *Journal of Food Engineering, 211*, 60–68. https://doi.org/10.1016/j.jfoodeng.2017.05.004

Wang, Q., Xie, Y., Xiong, Z., Gu, X., Nie, X., Lan, Y., & Chen, B. (2022). Structural and physical properties of spray-dried fish oil microcapsules via pea protein isolate based emulsification or complex coacervation with sugar beet pectin. *Journal of Food Engineering, 335*, Article 111173. https://doi.org/10.1016/j.jfoodeng.2022.111173

Yildiz, G., Ding, J., Gaur, S., Andrade, J., & Feng, H. (2018). Microencapsulation of docosahexaenoic acid (DHA) with four wall materials including pea protein-

modified starch complex. *International Journal of Biological Macromolecules, 114*, 935–941. https://doi.org/10.1016/j.ijbiomac.2018.03.175

Yu, Z., Yang, Y., Wang, C., Shi, G., Xie, J., Gao, B., … Shen, T. (2021). Nano-soy-protein microcapsule-enabled self-healing biopolyurethane-coated controlled-release fertilizer: Preparation, performance, and mechanism. *Materials Today Chemistry, 20*, Article 100413. https://doi.org/10.1016/j.mtchem.2020.100413

Zhu, L., Xu, Q., Liu, X., Xu, Y., & Liu, H. (2019). Oil-water interfacial behavior of soy β-conglycinin–soyasaponin mixtures and their effect on emulsion stability. *Food Hydrocolloids, 101*(3), Article 105531. https://doi.org/10.1016/j.foodhyd.2019.105531